Clinical Science (2016) **130**, 365–376 doi: 10.1042/CS20150609

Original Paper

Cardiomyocyte-specific overexpression of oestrogen receptor β improves survival and cardiac function after myocardial infarction in female and male mice

Iris Schuster*[1], Shokoufeh Mahmoodzadeh†‡[1], Elke Dworatzek‡§[1], Frédéric Jaisser‖, Smail Messaoudi‖, Ingo Morano† and Vera Regitz-Zagrosek‡§

*EA 2992, Medical University of Nîmes-Montpellier, Centre Hospitalo-Universitaire de Nîmes, Nîmes, France
†Max-Delbrueck-Center for Molecular Medicine in the Helmholtz Association, Berlin, Germany
‡DZHK (German Center for Cardiovascular Research), partner site Berlin, Berlin, Germany
§Institute of Gender in Medicine and Center for Cardiovascular Research, Charité Universitätsmedizin Berlin, Hessische Strasse 3-4, 10115 Berlin, Germany
‖Inserm, U872, Paris, France

Abstract

ERβ (oestrogen receptor β) activation has been shown to be cardioprotective, but the cell types and mechanisms involved are not understood. To investigate whether ERβ restricted to cardiomyocytes contributes to the observed cardioprotection, we tested the effects of cardiomyocyte-specific ERβ-OE (ERβ overexpression) on survival, cardiac remodelling and function after MI (myocardial infarction) and studied the molecular pathways potentially involved. Female and male mice with cardiomyocyte-specific ERβ-OE and WT (wild-type) littermates were subjected to chronic anterior coronary artery ligation or sham surgery. Two weeks after MI, ERβ-OE mice showed improved survival (100% and 83% compared with 76% and 58% in WT females and males respectively). ERβ-OE was associated with attenuated LV (left ventricular) dilatation, smaller increase in heart weight, less lung congestion at similar MI size, and improved systolic and diastolic function in both sexes. We identified two potential pathways for ERβ-mediated myocardial protection. First, male and female ERβ-OE mice had a lower reduction of SERCA2a (sarcoplasmic/endoplasmic reticulum Ca^{2+}-ATPase 2a) expression after MI, suggesting less reduction in diastolic Ca^{2+}-reuptake into the sarcoplasmic reticulum post-MI. Secondly, male ERβ-OE revealed attenuated cardiac fibrosis in the remote LV tissue and expression of fibrosis markers collagen I and III, periostin and *miR-21*. Cardiomyocyte-specific ERβ-OE improved survival associated with reduced maladaptive remodelling, improved cardiac function and less heart failure development after MI in both sexes. These effects seem to be related, at least in part, to a better maintenance of Ca^{2+} cycling in both sexes and a lower induction of cardiac fibrosis in males after MI.

Key words: cardiac function, fibrosis, myocardial infarction, oestrogen receptor β, sex differences

INTRODUCTION

Sex has an important impact on cardiac remodelling, which is defined as changes in structure, dimensions and physiology of the heart after injury [1]. In response to MI (myocardial infarction), women experience less adverse LV (left ventricular) remodelling than men, resulting in better preservation of LV size and function [2,3]. In animal models of MI, female mice showed improved survival, less maladaptive remodelling and better cardiac function compared with males [4]. These differences between sexes have been widely related to the sex hormone oestrogen. Oestrogen's effects are mainly mediated by two cognate receptors, ERα and ERβ (oestrogen receptor α and β), which are expressed in the myocardium of males and females in a broad variety of

Abbreviations: EF, ejection fraction; ER, oestrogen receptor; ERβ-OE, ERβ overexpression; ERK1/2, extracellular-signal-regulated kinase 1/2; HF, heart failure; LV, left ventricular; LVEDV, LV end-diastolic volume; LVESV, LV end-systolic volume; MI, myocardial infarction; PLN, phospholamban; SERCA2, sarcoplasmic/endoplasmic reticulum Ca^{2+}-ATPase 2; SR, sarcoplasmic reticulum; TDI, tissue Doppler imaging; WT, wild-type.

[1] These authors contributed equally to this work.

Correspondence: Dr Elke Dworatzek (email Elke.Dworatzek@charite.de).

species ranging from mice to humans [5–8]. Although both ER subtypes activate a variety of signal transduction pathways [9,10], functions of the individual ER subtypes are still not completely understood. The development of transgenic and knockout animal models has helped so far to elucidate this important issue.

Studies using mouse models to analyse the role of ER in MI pointed to a protective role of ERβ in female mice. Pelzer et al. [11] showed increased mortality and aggravated clinical and biochemical markers of HF (heart failure) in systemic ERβ-knockout (ER$\beta^{-/-}$) female mice after experimental MI. Korte et al. [12] observed impaired repolarization and automaticity in female mice post-MI, and Babiker et al. [13] observed increased MI size among female ER$\beta^{-/-}$ mice.

The molecular basis for the observed cardioprotective effects of ERβ after MI needs further investigation. Pelzer et al. [11] observed an impairment of Ca^{2+}-handling proteins in female ER$\beta^{-/-}$ mice. In a model of pressure overload using systemic ER$\beta^{-/-}$ mice, we showed previously that ERβ attenuates the development of LV fibrosis [14].

Furthermore, activation of specific myocardial hypertrophy-associated signalling pathways has been shown to be cardioprotective [15]. For instance, increased PI3K (phosphoinositide 3-kinase)/Akt activity led to improved survival in a mouse model of dilated cardiomyopathy and to favourable effects on cardiac function and remodelling [16,17]. We and others have shown that cardioprotective signalling pathways are modulated by ERβ [18,19].

The effects of ERβ in the male sex after MI have not yet been studied. Furthermore, using systemic knockout models, it has not been clarified whether systemic or cardiac-specific effects of ERβ confer cardioprotection. In the present study, we therefore used a cardiomyocyte-specific ERβ-OE (ERβ overexpression) mouse model which allowed the analysis of cardiac effects of ERβ independently of systemic effects on both sexes subjected to MI. The main hypothesis of the present study was that a cardiomyocyte-specific ERβ-OE attenuates pathological myocardial remodelling and preserves cardiac function after MI in both sexes.

MATERIALS AND METHODS

Generation of transgenic mice

A novel transgenic mouse model with cardiomyocyte-specific ERβ-OE was generated. Inducible double-transgenic mice with cardiomyocyte-specific ERβ-OE were generated through mating of monotransgenic mouse ERβ (tetO-mERβ) and monotransgenic β-MHC-tTA mice using the Tet-Off system (see the Supplementary Online Data for details). Male and female ERβ-OE and WT (wild type) littermate mice with B6D2F background were used.

Induction of myocardial infarction

Experiments were conducted in accordance with the Guide for the Care and Use of Laboratory Animals published by the U.S. National Institutes of Health (NIH Publication Number 85-23, revised 2011) and with the guidelines of the State Agency for Health and Social Affairs (LaGeSo, Berlin, Germany, G0246/12). Female and male ERβ-OE and WT littermates aged 10–12 weeks were randomly assigned to MI or sham surgery. MI was induced in female and male mice by permanent left anterior descending coronary artery ligation. Briefly, after induction of anaesthesia (ketamine hydrochloride at 80 mg/ml and xylazine hydrochloride at 12 mg/ml by intraperitoneal injection at a dose of 1 mg/kg), mice were intubated and ventilated (respirator: Ugo Basile model; FMI). After exposing the left anterior descending coronary artery through a fourth intracostal left lateral thoracotomy, the artery was permanently ligated with a 7.0 polypropylene suture at a distance of 1–2 mm from the left auricle. Sham animals underwent the same surgical procedure, but the ligature was not tied. Animals were treated with rimadyl (5 mg/kg) for analgesia up to 7 days post-surgery.

High-resolution echocardiography

Echocardiography was performed under isoflurane anaesthesia 1 day before and 2 weeks after surgery with a Vevo 770 instrument (VisualSonics) [14] equipped with a 20–55 MHz transducer. Anaesthesia was induced with 3% isoflurane and maintained with 1.5% isoflurane. Body temperature was maintained through a heating pad at 37 °C. Electrocardiogram and respiration were monitored during echocardiography. Images and cineloops were acquired for further offline analysis by a single operator blinded for genotype, sex and operation. LVEDV (LV end-diastolic volume) and LVESV (LV end-systolic volume), mean wall thickness and EF (ejection fraction) were determined by tracing of endocardial and epicardial borders and majors in end-diastole and in end-systole in the parasternal long axis view. Transmitral flow analysis from the four chamber view was used to characterize diastolic function from the following parameters: peak E and A waves, E wave deceleration time and filling interval. Pulsed-wave Doppler measurements were made at the ascending aorta level for the determination of ejection time and LV pre-ejection time, and at the origin of the pulmonary artery for the determination of right ventricular pre-ejection time. The difference between the electromechanical ejection delay of the LV (duration from the QRS complex to the beginning of the aortic outflow) and of the right ventricular (duration from de QRS complex to the beginning of the pulmonary outflow) was used as an index of interventricular asynchrony [20]. TDI (tissue Doppler imaging) systolic S and diastolic E′ wave from the septal side of the mitral annulus were measured and the ratio transmitral E to mitral annulus E′ was calculated. The myocardial performance index [(filling interval−ejection time)/ejection time] was calculated as an index of global systolic and diastolic function.

Infarct size determination

MI size was determined by echocardiography based on LV wall motion according to the method used in clinical routine in humans [21]. Since the development of high-resolution ultrasound machines, echocardiographic analysis is recognized as a precise and non-invasive evaluation technique for LV morphology and function in small animals [22,23]. An additional advantage is the preservation of LV tissue for molecular analysis in the same cohort of animals. Echocardiographic evaluation of MI size has been

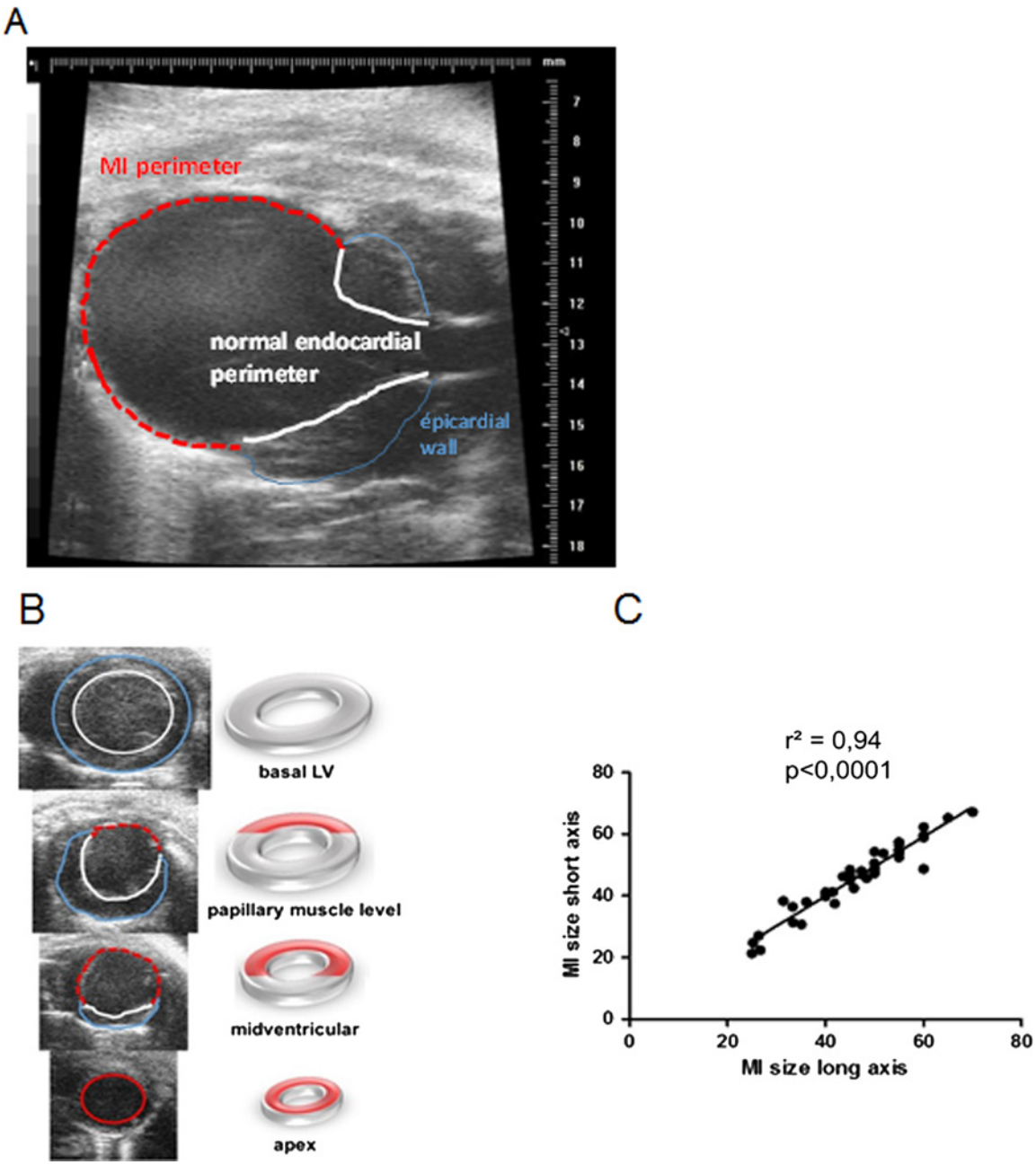

Figure 1 **Echocardiographic MI size determination**
Example of MI size determination from (**A**) the long axis view and (**B**) the short axis view. (**C**) Correlation between MI size determination from long and short axis views.

shown to strongly correlate with histological determination ($r = 0.96$) [24] and with LV systolic dysfunction ($r = 0.94$) [25]. We used the Electrocardiogram-Gated Kilohertz Visualization™-mode which synthesizes high temporal resolution B-Mode images by combining electrocardiogram-synchronized heart cycles, thus producing sequences at up to 1000 frames/s. The synthesized cycle was displayed in slow motion before tracing endocardial perimeters at end diastole. As shown in Figure 1(A), MI size was determined from the long axis view obtained with high definition in mice. MI size (%) was calculated [24] as the internal perimeter of the infarcted region, identified by a thinned akinetic wall, in relation to the total perimeter of the LV cavity: MI (%) = MI perimeter/(MI perimeter+normal endocardial perimeter)×100. For comparison, MI size was also determined as the mean from four different short axis views at basal, papillary, mid-ventricular and apical LV level (Figure 1B) which show horizontal views of the ventricle. Figure 1(C) shows a high correlation between MI size determined from long and short axis

views ($r^2 = 0.94$; $P < 0.0001$, $n = 67$). As small infarcts induce no global or only minimal regional remodelling, only animals with an MI size >20% in the MI groups were included.

Tissue sampling

Mice that died before the end of the observation period were subjected to autopsy, and heart and lungs were examined. At 2 weeks after MI, surviving mice were anaesthetized with 1.5% isoflurane and killed by cervical dislocation. Hearts were harvested, left ventricles were isolated and immediately snap-frozen in liquid nitrogen and stored at −80 °C or fixed in 4% (w/v) formaldehyde for at least 24 h until use for gene and protein or histological analyses.

Cell morphology

Adult mouse ventricular cardiomyocytes were isolated as described previously [26]. Individual length and width of the cardiomyocytes were determined on micrographs captured using an Axiovert 40 CFL microscope (using objective: N-Achroplan ×10/0.25 Ph1 W 0.8) and digitized by AxioCam MR3 camera. Ten micrographs per sample were taken randomly, and 300–500 rod-shaped myocytes were measured per sex and genotype. Length and width of cardiomyocytes were determined at the widest point of each cell using the program AxioVision Release 4.8 (Zeiss).

Quantitative real-time PCR

Total RNA isolation from LV tissue and quantitative real-time PCR were conducted as described previously [14,18]. The primers used for quantification of relative gene expression of mouse *Col1A2* and *Col3A1* (collagens I and III), *NPPA* (atrial natriuretic peptide A), *Myh6* (myosin heavy chain 6), *Myh*7, *miR-21*, *miR-24*, *miR-27a* and *miR-106a* are listed in Supplementary Table S1. Gene expression levels were normalized to *RPLO* (50S ribosomal protein L15) and the amount of miRNAs was normalized using the average of the expression of *RNU6B* (U6 small nuclear RNA) and *RNU1A*.

Western blot analysis

Analysis was performed as described previously [6]. Primary antibodies were used against the following: ERα (G-20, Santa Cruz Biotechnology), ERβ (SP5198P, Acris), periostin (S-15, Santa Cruz Biotechnology), SERCA2 (sarcoplasmic/endoplasmic reticulum Ca^{2+}-ATPase 2) (ATP2A2/SERCA2a, SM5113, Acris), PLN (phospholamban) (SAB2701037, Sigma–Aldrich), p-PLN (sc-17024-R, Santa Cruz Biotechnology), p-p44/p42 ERK1/2 (extracellular-signal-regulated kinase 1/2) (Thr^{202}/Tyr^{204}) (#4370, Cell Signaling Technology), p44/p42 ERK1/2 (#4695, Cell Signaling Technology), phospho-Akt1/2/3 (Ser^{473}-R, Santa Cruz Biotechnology), Akt1/2/3 (H-136, Santa Cruz Biotechnology), α-tubulin (clone DM1A, Sigma–Aldrich) and GAPDH (glyceraldehyde-3-phosphate dehydrogenase) (MAB374, Millipore).

Histological analysis and immunofluorescence

LV sections were stained with Sirius Red to determine collagen deposition as described previously [18]. Fibrosis in remote areas was calculated as the ratio of fibrotic area (excluding the MI zone) to total myocardial area in the remote zone. For immunofluorescence, paraffin-embedded sections were incubated with anti-mouse ERβ antibody (SP5198P, Acris) followed by secondary FITC-conjugated anti-mouse IgG (Jackson ImmunoResearch Laboratories), as described previously [7]. Nuclei were stained with DAPI. Confocal images were acquired using a Leica TCS-SPE spectral confocal laser-scanning microscope.

Statistical analysis

Data are shown as means ± S.E.M. The differences between groups were tested using ANOVA as appropriate. Three-way ANOVA was used to analyse interactions between operation, genotype and sex, followed by Fisher's PLSD (partial least-squares difference) post-test to independently assess the overall effect of operation (MI compared with sham), genotype (ERβ-OE compared with WT) or sex (male compared with female). Two-way ANOVA was used to test the influence of operation independently of genotype, and of genotype independently of sex, followed by Bonferroni's post-hoc test using GraphPad Prism 5.01. MI mortality was illustrated by Kaplan–Meier curves and analysed by log-rank test. Peri-procedural deaths within the first 24 h of the operation were excluded. $P \leqslant 0.05$ was considered statistically significant.

RESULTS

Characterization of ERβ-OE mice

There were no differences in heart weight, LV morphology, cardiac function (Supplementary Table S2) or cardiomyocyte size (Figure 2A) between ERβ-OE and WT mice at basal level. ERβ protein was significantly higher in whole protein lysate from LV of ERβ-OE compared with WT mice (female, 1.8-fold; male, 1.5-fold; Figure 2B). ERβ-OE in the LV was confirmed by immunofluorescence (Figure 2C). ERβ-OE was specific to the heart, and ERβ expression did not increase in kidney, soleus and uterus of ERβ-OE mice (Supplementary Figure S1). There was no change in ERα protein expression in LV tissues (Figure 2D). Blood serum oestradiol levels were not different between ERβ-OE and WT mice (Supplementary Results section).

ERβ-OE reduces mortality rate after myocardial infarction

ERβ-OE significantly reduced mortality compared with WT mice after MI ($P = 0.008$; Figure 3). The survival rate 2 weeks after MI was 100% and 83% in ERβ-OE and 76% and 58% in WT female and male mice respectively. Female and male WT mice that died before the end of the observation period showed 25% and 50% of cardiac rupture respectively, with a peak at day 3.8 ± 0.8, whereas no rupture was observed in ERβ-OE mice. Cardiac rupture was indicated by blood coagula in the chest cavity and small slits commonly observed at the LV free wall. After day 4, only female and male WT mice died, showing signs of pulmonary congestion at autopsy.

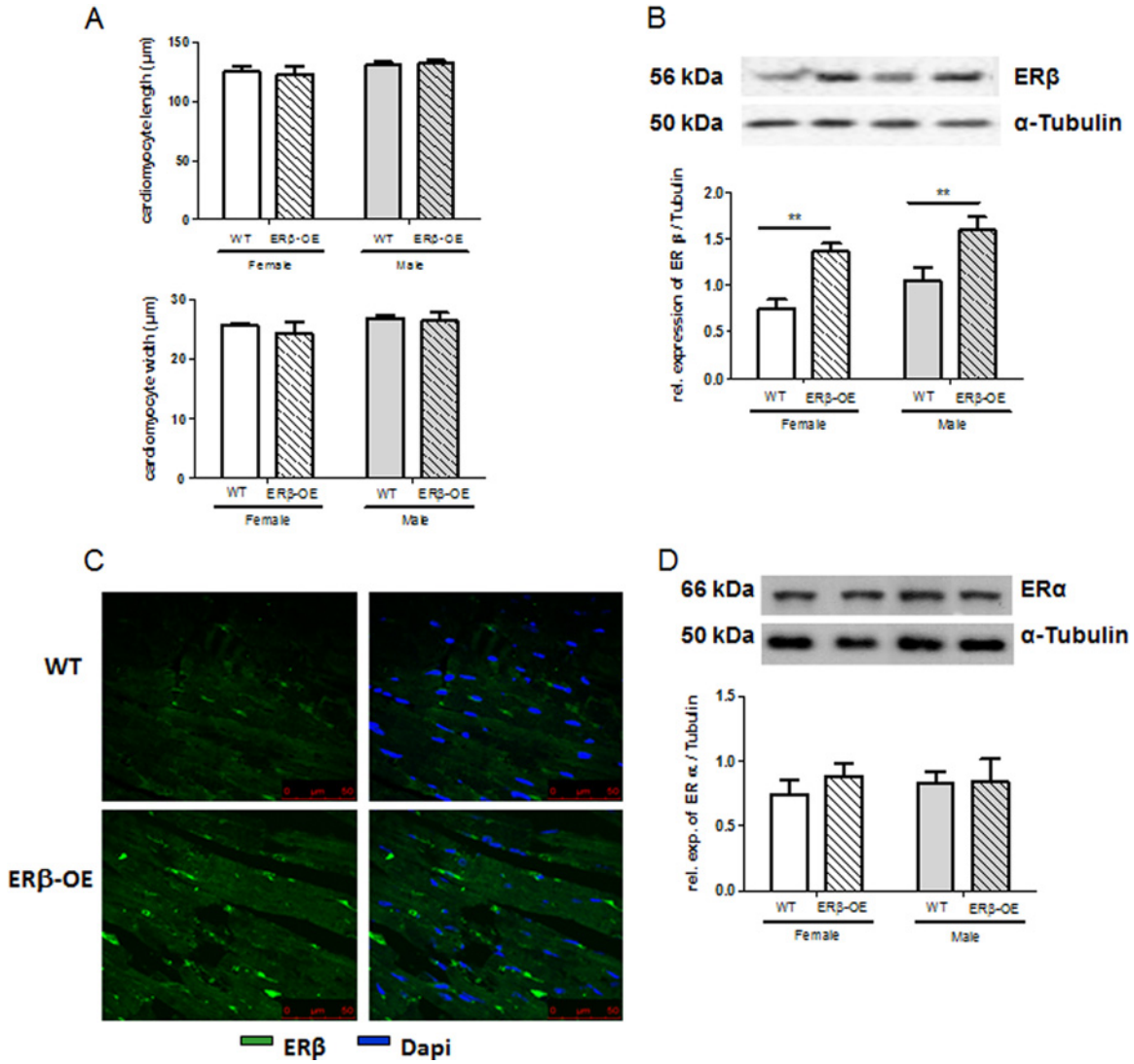

Figure 2 **Characterization of ERβ-OE mice**

(**A**) Diastolic cardiomyocyte length and width are not different between ERβ-OE and WT mice. Results are means ± S.E.M. for 100–300 cells/group. (**B**) ERβ protein level is higher in LV tissue of female and male ERβ-OE than in WT mice ($n \geqslant 7$/group), two-way ANOVA: $P < 0.01$ for both groups (genotype effect: ERβ-OE compared with WT). (**C**) Immunofluorescence of ERβ (green) in cardiomyocytes of ERβ-OE and WT. Nuclei are stained blue (DAPI). Magnification ×20; scale bar, 250 µm. (**D**) ERα protein level is not changed by ERβ-OE overexpression. Tubulin was used as control. Results are means ± S.E.M. ($n \geqslant 7$/group). Molecular masses are indicated in kDa.

ERβ-OE attenuates LV maladaptive remodelling

After MI, LV mean wall thickness was reduced due to the thinned infarcted myocardial wall, whereas LV volumes increased (Table 1). ERβ-OE did not affect MI size, but was associated with reduced LV maladaptive dilatation. ERβ-OE mice had a smaller increase in LVEDV and LVESV with a sex–genotype–surgery interaction for both parameters after MI (Table 1). ERβ-OE was also associated with a smaller increase in heart and lung weight normalized for tibia length with a genotype–surgery interaction. WT mice had not only higher heart, but also higher lung weight, indicating a more advanced stage of HF compared with ERβ-OE. Separate analysis in each sex after MI showed a significant ERβ-OE effect on LV volumes only in males (Figure 4A).

ERβ-OE preserves LV systolic and diastolic function after MI

MI surgery significantly reduced parameters of systolic and diastolic function (Table 1). ERβ-OE was associated with a smaller decrease in EF, TDI S wave and with lower interventricular asynchrony in both sexes. ERβ-OE mice also showed a better preserved diastolic function after MI, as indicated by TDI E wave, E wave deceleration time, E/E′ ratio and a better preservation of myocardial performance index. A genotype–surgery interaction was observed for all functional parameters. Separate analysis in each sex after MI showed a significant ERβ-OE effect on TDI S and diastolic parameters in both sexes (Figure 4B), whereas the effect on EF was only significant in males (Figure 4A).

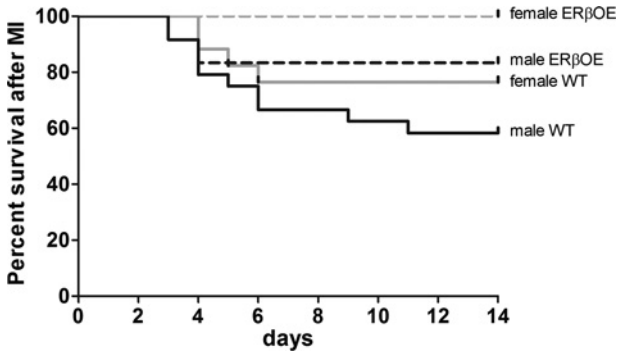

Figure 3 Survival curves of ERβ-OE and WT mice
Kaplan–Meier curves of female ERβ-OE (broken grey line; $n = 18$), male ERβ-OE (broken black line; $n = 12$), female WT (continuous grey line; $n = 17$) and male WT (continuous black line; $n = 24$). Genotype effect: ERβOE compared with WT; $P = 0.008$.

Effect of ERβ-OE on hypertrophy markers after MI

MI significantly induced *NPPA* mRNA in the LV remote area compared with sham (MI compared with sham; $P < 0.0001$). Separate analysis in each sex after MI showed that ERβ-OE significantly attenuated *NPPA* expression after MI only in male mice (Supplementary Figure 2A). *Myh6*/*Myh7* ratio revealed no significant change after MI (Supplementary Figure 2B). Furthermore, measurement of signalling pathways involved in cardioprotection [17,27], i.e. phosphorylation of Akt (p-Akt) and ERK1/2 (p-ERK1/2) showed no significant changes after MI (Supplementary Figures 2C and 2D).

ERβ-OE attenuates the development of cardiac fibrosis and the expression of fibrosis markers

MI induced an increase in cardiac fibrosis in the LV remote area associated with increased expression of *Col I* and *Col III* mRNA, *miR-21* and periostin protein (MI compared with sham; $P < 0.0001$ for all parameters). ERβ-OE was associated with lower fibrosis and reduced expression of *Col I* and *III* (ERβ-OE compared with WT; $P < 0.05$ for all three parameters). Separate analysis in each sex after MI showed that the ERβ-OE effect on fibrosis, *Col I* and *Col III* reduction was significant only in males (Figure 5A–5D). In addition, *miR-21* expression and periostin protein were not significantly increased in male ERβ-OE compared with male WT after MI (Figures 5E and 5F). Levels of *miR-24*, *miR-27a* and *miR-106a* revealed no significant alteration after MI (Supplementary Figure S3). Inflammatory marker levels (interleukin 6, tumour necrosis factor α, TYRO protein tyrosine kinase-binding protein and Fc receptor IgE high-affinity I γ polypeptide-targeted mutation 1) were not significantly different between ERβ-OE and WT mice two weeks post-MI (results not shown).

ERβ-OE improves the expression of Ca^{2+}-handling proteins

MI significantly reduced SERCA2a protein expression in the LV remote area compared with sham ($P < 0.0001$). ERβ-OE was associated with significantly higher expression of SERCA2a compared with WT ($P < 0.0001$). Separate analysis in each sex showed that SERCA2a levels were significantly higher in female and male ERβ-OE compared with WT after MI (Figure 6A). The ratio of phosphorylated PLN to total PLN showed no significant difference between MI groups (Figure 6B).

DISCUSSION

Cardioprotective effects of ERβ, particularly in females, have been reported. However, mechanistic understanding is limited and it was not possible to separate ERβ systemic effects from cardiac effects. We now show for the first time that cardiomyocyte-specific ERβ-OE led to improved survival, reduced LV remodelling and better cardiac function in male and female mice 2 weeks after MI.

ERβ-OE effect on survival

Cardiomyocyte-specific ERβ-OE significantly improved survival 2 weeks after MI. Interestingly, we observed no LV rupture in ERβ-OE mice during the early phase after MI. This might be associated with decreased early LV remodelling and inflammation. However, the present study was not an acute study and 2 weeks after MI, we could not show any difference in inflammatory markers. The investigation of mechanisms associated with the reduction of rupture by ERβ-OE will be of high interest for future studies. In contrast with WT mice, all ERβ-OE mice survived after day 4. No HF -associated deaths were observed in ERβ-OE animals and this can be related to reduced LV remodelling and to improved systolic and diastolic function. Long-term pro-survival effects of ERβ in female mice have also been suggested by loss-of-function studies with increased mortality in female $ER\beta^{-/-}$ mice [11–14], associated with an increase in HF markers [11]. Data from the present study show improved survival after MI in females by ERβ-OE, underscoring the beneficial role of ERβ in females. However, our findings on improved survival by ERβ-OE in males are completely novel, and may reveal an interesting pathway for cardioprotection in males. In contrast with studies with systemic modulation of ERβ, the present study is based on a cardiomyocyte-specific approach. We can thus exclude the contribution of systemic effects.

ERβ-OE effect on MI size, LV remodelling and cardiac function

Improved survival and reduced maladaptive remodelling in ERβ-OE mice were not related to a different MI size compared with WT. These results are in accordance with previous studies of Korte et al. [12] and Pelzer et al. [11] who observed no change in MI size in $ER\beta^{-/-}$ females. After MI, ERβ-OE in cardiomyocytes induced a smaller increase in LVEDV and LVESV, and a smaller decrease in EF compared with WT. Parameters of myocardial function such as TDI S and E′ wave, reflecting intrinsic myocardial relaxation and contraction, showed a significantly better preservation in ERβ-OE mice. ERβ-OE was also associated with a lower increase in interventricular asynchrony. Cardiac asynchrony, due to asynchronous contraction between the right ventricle and the infarcted LV, is an important prognostic marker in patients after MI for survival, cardiac remodelling and

Table 1 LV echocardiographic data and organ weight 2 weeks after myocardial infarction or sham surgery in female and male WT and ERβ-OE mice

Results are means ± S.E.M. ANOVA analysis for surgery (MI compared with sham), genotype (ERβ-OE compared with WT) and sex effect (male compared with female). Interaction analysis between factors: *genotype–operation interaction and †sex–genotype–operation interaction $P < 0.05$. TL, tibia length; TDI S, TDI of the systolic S wave at the septal border of the mitral annulus; TDI E′, TDI of the diastolic E′ wave at the septal border of the mitral annulus; EWDT, E wave deceleration time.

	Female WT sham ($n = 17$)	Female WT MI ($n = 13$)	Male WT sham ($n = 18$)	Male WT MI ($n = 14$)	Female ERβ-OE sham ($n = 18$)	Female ERβOE MI ($n = 18$)	Male ERβ-OE sham ($n = 15$)	Male ERβ-OE MI ($n = 10$)	MI effect	Sex effect	ERβ effect	Interaction
Heart rate (beats/min)	460 ± 3	479 ± 4	457 ± 3	480 ± 5	454 ± 5	479 ± 4	457 ± 4	476 ± 3	<0.0001	NS	NS	
MI size (%)	47 ± 1	–	51 ± 2	–	45 ± 1	–	47 ± 3	–	NS	NS		
LV morphology												
Mean wall thickness (mm)	0.65 ± 0.01	0.56 ± 0.01	0.66 ± 0.01	0.55 ± 0.02	0.67 ± 0.01	0.56 ± 0.02	0.68 ± 0.01	0.57 ± 0.02	<0.0001	NS	NS	
LVEDV (μl)	53 ± 2	77 ± 2	67 ± 2	110 ± 9	48 ± 1	72 ± 5	64 ± 2	83 ± 4	<0.0001	<0.0001	<0.001	*†
LVESV (μl)	18 ± 1	52 ± 3	24 ± 1	81 ± 9	16 ± 1	47 ± 5	21 ± 2	51 ± 4	<0.0001	<0.001	<0.001	*†
Systolic function												
EF (%)	65 ± 1	34 ± 2	66 ± 2	26 ± 2	67 ± 1	39 ± 2	66 ± 2	40 ± 3	<0.0001	NS	0.01	*†
TDI S ($cm \cdot s^{-1}$)	24 ± 1	16 ± 1	26 ± 1	15 ± 1	25 ± 1	20 ± 1	26 ± 1	20 ± 1	<0.0001	NS	0.01	*
Asynchrony Index (ms)	0.6 ± 0.1	3.4 ± 0.3	0.7 ± 0.1	5.0 ± 0.9	0.6 ± 0.1	2.0 ± 0.3	0.8 ± 0.2	3.1 ± 0.2	<0.0001	<0.01	<0.01	*
Diastolic function												
EWDT time (ms)	28 ± 1	17 ± 1	30 ± 2	13 ± 1	30 ± 1	22 ± 1	30 ± 2	19 ± 2	<0.0001	NS	0.01	*
TDI E′ ($cm \cdot s^{-1}$)	33 ± 1	23 ± 1	35 ± 1	20 ± 1	34 ± 1	28 ± 1	33 ± 1	28 ± 1	<0.0001	NS	0.01	*
E/E′ ratio	26 ± 1	36 ± 2	25 ± 1	37 ± 2	25 ± 2	29 ± 2	26 ± 1	27 ± 1	<0.0001	NS	<0.01	*
Myocardial performance index	0.27 ± 0.02	0.74 ± 0.04	0.29 ± 0.03	0.90 ± 0.10	0.31 ± 0.02	0.55 ± 0.05	0.29 ± 0.02	0.69 ± 0.06	<0.0001	NS	<0.05	*
Organ weight (μg/mm)												
Heart weight/TL	6.5 ± 0.02	9.2 ± 0.04	8.5 ± 0.03	11.7 ± 0.10	6.9 ± 0.02	8.4 ± 0.05	8.6 ± 02	9.9 ± 0.06	<0.0001	<0.0001	<0.01	*
Lung weight/TL	8.0 ± 0.1	9.5 ± 0.2	8.5 ± 0.2	10.7 ± 0.5	8.2 ± 0.1	8.6 ± 0.2	8.5 ± 0.2	9.8 ± 0.4	<0.0001	<0.0001	<0.05	*
Liver weight/TL	59 ± 3	66 ± 2	72 ± 2	79 ± 4	60 ± 2	61 ± 1	73 ± 3	75 ± 3	NS	<0.0001	<0.05	
Uterus weight/TL	5.0 ± 0.6	5.4 ± 0.5	–	–	5.2 ± 0.4	5.3 ± 0.5	–	–	NS	<0.0001	<0.05	

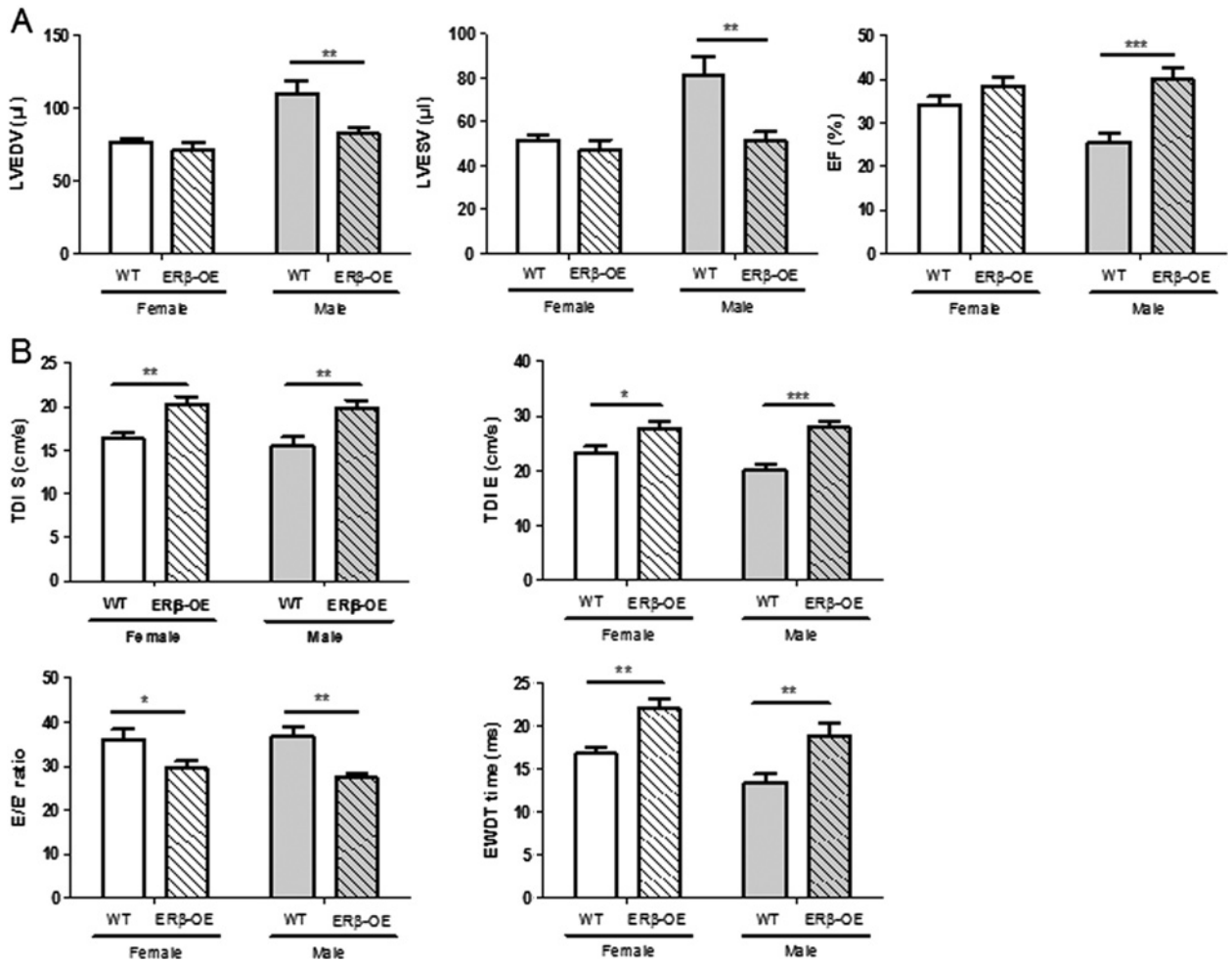

Figure 4 Effect of ERβ-OE on LV morphology and function in MI groups

(**A**) Effect on LV volumes and EF. (**B**) Effect on parameters of intrinsic myocardial systolic and diastolic function (TDI S, TDI E, E/E′ ratio, E wave deceleration time). Two-way ANOVA for sex and genotype in MI groups: $*P < 0.05$, $**P < 0.01$ and $***P < 0.001$. Results are means ± S.E.M.; $n \geqslant 12$ per group.

function [20]. Diastolic parameters such as E wave deceleration time and the E/E′ ratio were significantly less impaired in ERβ-OE mice, indicating less increased LV filling pressures. This is in agreement with the observation of lower lung weight in ERβ-OE, suggesting attenuated HF compared with WT. Finally, the myocardial performance index, a global marker of systolic and diastolic function, was significantly less increased in ERβ-OE, indicating higher global efficiency.

Although most of these functional parameters were improved in females and males by ERβ-OE, the effect on LV volumes and on EF was more pronounced in males than in females. This difference seems to be due, at least in part, to the fact that male WT showed worse maladaptive remodelling and thus benefited most from ERβ-OE.

Molecular mechanism of ERβ-induced cardioprotection

The present study identified two molecular pathways by which ERβ might contribute to cardioprotection. First, we observed a lower reduction of SERCA2a protein expression in male and female ERβ-OE after MI compared with WT mice. In human and experimental HF, a diminished Ca^{2+} uptake resulting from decreased expression/activity of SERCA2a is recognized as a hallmark of HF [28]. In cardiomyocytes, SERCA2a plays a central role in Ca^{2+} cycling required for both relaxation and contraction [29]. SERCA2a transports Ca^{2+} from the cytosol into the SR (sarcoplasmic reticulum), thereby contributing to the low diastolic Ca^{2+} levels required for relaxation and replenishing Ca^{2+} stores needed for the next contraction [30]. Although SERCA2a homozygous knockout ($SERCA2a^{-/-}$) mice die early in development, heterozygous SERCA2a ($SERCA2a^{+/-}$) mice showed decreased myocyte contractility and SR Ca^{2+} load, resulting in HF in combination with an increased haemodynamic load [31,30]. On the other hand, SERCA2a overexpression in the heart of transgenic mice accelerates Ca^{2+} transients and cardiac relaxation resulting in higher cardiac contractility [32,33]. In the present study, a better reuptake of Ca^{2+} from the cytosol to the SR via an increased expression of the Ca^{2+}-ATPase during diastole might explain a

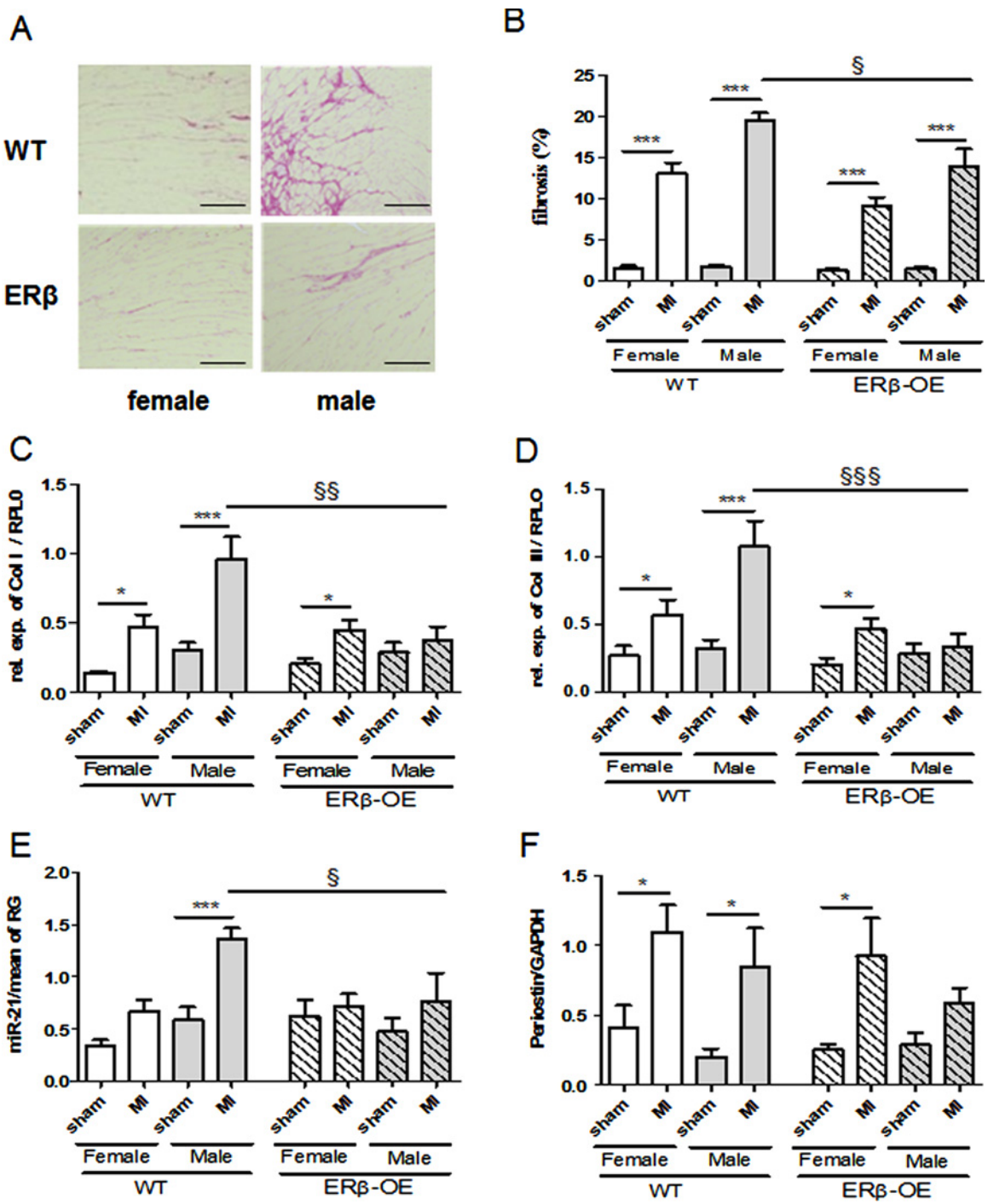

Figure 5 **ERβ-OE attenuates fibrosis in male mice**

(**A**) Representative images of Sirius Red-stained LV tissues from female and male WT and ERβ-OE mice after MI (remote area). Magnification ×10; scale bar, 200 μm. (**B**) Percentage of fibrosis in LV remote area. (**C**) *Col I*, (**D**) *Col III* mRNA, (**E**) *miR-21* expression, (**F**) periostin protein. For all analyses, two-way ANOVA was used. MI-effect independent of genotype: $*P < 0.05$ and $***P < 0.001$; genotype effect independent of sex: §$P < 0.05$, §§$P < 0.01$ and §§§$P < 0.001$. Results are means ± S.E.M.; $n \geqslant 8$/group.

better myocardial relaxation, as indicated by improved TDI E′ in ERβ-OE compared with WT mice. Increased SR Ca^{2+} content due to higher SERCA2a expression might in turn explain a more important Ca^{2+} release via the ryanodine receptors and an increase in the Ca^{2+} transient during systole. This could contribute to better intrinsic contraction as indicated by improved TDI S and better global myocardial performance as observed in ERβ-OE males and females. Improved Ca^{2+} cycling between SR and

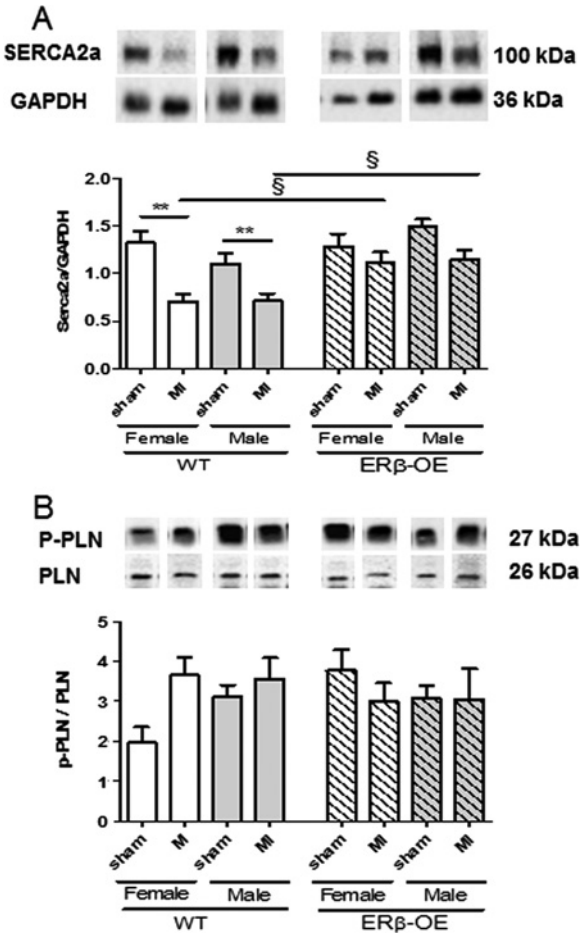

Figure 6 ERβ-OE improves the expression of Ca^{2+}-handling protein

(**A**) SERCA2a and (**B**) p-PLN/PLN protein expression. Results are means ± S.E.M.; $n \geqslant 8$/group. For analysis, two-way ANOVA was used. MI-effect independent of genotype: $^{**}P < 0.01$; genotype effect independent of sex: $^{\S}P < 0.05$.

the cytosol might thus constitute a mechanism of cardioprotection mediated by ERβ.

Secondly, reduced maladaptive remodelling observed with ERβ-OE was associated with lower cardiac fibrosis and expression of fibrosis markers after MI, particularly in male mice. Post-infarct LV remodelling is due to infarct expansion but also to remodelling processes in the remote zone. Although healing of the infarct zone with a firm fibrous scar is essential for chamber integrity, exaggerated fibrosis in the remote zone can lead to maladaptive remodelling, thus contributing to cardiac dysfunction [34]. Attenuated cardiac fibrosis in male ERβ-OE animals might be therefore one underlying reason for significantly less maladaptive remodelling and better EF (as a volume-dependent parameter). ERβ-OE in female hearts did not attenuate fibrosis after MI compared with female WT, which might be due to the fact that females develop less fibrosis compared with male WT-mice [14]. Furthermore, Pelzer et al. [11] also showed no ERβ-mediated modulation of the myocardial collagen content in female $ER\beta^{-/-}$ animals compared to WT females after MI. Sex-specific anti-fibrotic effects of ERβ have already been described in different mouse models, e.g. pressure overload induced myocardial hypertrophy. Our previous studies showed ERβ-mediated sex-specific cardiac remodelling in a pressure overload-induced mouse model and in miRNA regulation involved in cardiac fibrosis development [14,35].

Reduced fibrosis and expression of fibrosis markers in male ERβ-OE mice may be mediated by reduction of *miR-21* expression. Silencing of *miR-21* in different HF models led to the suppression of cardiac fibrosis, collagen and periostin expression and attenuation of cardiac dysfunction [36–38]. ERβ-mediated down-regulation of *miR-21* has been described by us and others [35,39] and could contribute to anti-fibrotic effects in male ERβ-OE mice. These data indicate that ERβ plays an important role in the development of fibrosis in male sex after MI.

Study limitations

An overexpression model, as a gain-of-function model, does not exactly reflect the ERβ effect in a physiological setting. However, it may illustrate the potential effects of specific ERβ agonists on cardiomyocytes. Further studies are necessary to study the effects of ERβ in the setting of acute MI, including, in particular, the pathways associated with LV rupture during the early phase post-MI, which was reduced by ERβ-OE. Although our model was based on a cardiomyocyte-specific approach, we cannot exclude the involvement of other cardiac cell types. Cellular cross-talk between cardiomyocytes and fibroblasts in particular might have contributed to the observed effects on fibrosis. Further mechanistic studies are necessary to investigate the role of this cellular cross-talk.

CLINICAL PERSPECTIVES

- The lower incidence of ischaemic cardiomyopathy in pre-menopausal women compared with age-matched men raises the crucial question about the mechanisms of oestrogen- and oestrogen receptor-mediated cardioprotection, which is incompletely understood. In experimental models, ERβ activation has been shown to be cardioprotective, but the cell types and mechanisms involved are unclear.
- In the present study, cardiomyocyte-specific overexpression of ERβ in the setting of chronic MI induced improved survival in mice of both sexes and was associated with less maladaptive LV remodelling, better cardiac function and less HF development.
- Overexpression of ERβ in cardiomyocytes conferred significant cardioprotective effects, which may lead to the development of therapies that selectively enhance beneficial ERβ effects in female and male hearts. Subtype-selective oestrogen receptor modulators are already used in clinical practice or are currently tested for the treatment of breast cancer and osteoporosis [40] and may also be of interest in the treatment of cardiac diseases.

AUTHOR CONTRIBUTION

Iris Schuster performed experiments, data acquisition and analysis, and was involved in writing the paper. Shokoufeh Mahmoodzadeh designed and planned the study, performed experiments, data acquisition and analysis, and was involved in writing the paper. Elke Dworatzek performed experiments, data acquisition and analysis, and was involved in writing the paper. Frédéric Jaisser generated monotransgenic ERβ and monotransgenic tTA mice, and contributed to discussion and critical revision of the paper. Smail Messaoudi generated monotransgenic ERβ and monotransgenic tTA mice, and contributed to discussion and critical revision of the paper. Ingo Morano isolated cardiomyocytes, evaluated cardiomyocyte size, and contributed to discussion and critical revision of the paper. Vera Regitz-Zagrosek designed and planned the study and was involved in writing the paper.

ACKNOWLEDGEMENTS

We thank V. Riese, A. Kühne, B. Fielitz and P. Domaing for technical support, Dr P.A. Furth (Georgetown University, Washington, DC) for providing the mERβ construct and Professor Dr G. Schuler (Justus-Liebig-Universität Gießen, Frankfurter Straße) for oestradiol measurements in mouse blood samples.

FUNDING

This work was supported by the Deutsche Forschungsgemeinschaft [grant number FOR1054 (to V.R.-Z. and S.M.)], the German Center for Cardiovascular Research (DZHK) [grant number 81Z3100232 (to V.R.-Z.), and the Fédération Française de Cardiologie (to I.S.).

REFERENCES

1 Piro, M., Della Bona, R., Abbate, A., Biasucci, L.M. and Crea, F. (2010) Sex-related differences in myocardial remodeling. J. Am. Coll. Cardiol. **55**, 1057–1065 CrossRef PubMed

2 Dunlay, S.M. and Roger, V.L. (2012) Gender differences in the pathophysiology, clinical presentation, and outcomes of ischemic heart failure. Curr. Heart Fail. Rep. **9**, 267–276 CrossRef PubMed

3 O'Meara, E., Clayton, T., McEntegart, M.B., McMurray, J.J., Pina, I.L., Granger, C.B., Ostergren, J., Michelson, E.L., Solomon, S.D., Pocock, S. et al. (2007) Sex differences in clinical characteristics and prognosis in a broad spectrum of patients with heart failure: results of the Candesartan in Heart failure: Assessment of Reduction in Mortality and morbidity (CHARM) program. Circulation **115**, 3111–3120 CrossRef PubMed

4 Cavasin, M.A., Tao, Z., Menon, S. and Yang, X.P. (2004) Gender differences in cardiac function during early remodeling after acute myocardial infarction in mice. Life Sci. **75**, 2181–2192 CrossRef PubMed

5 Grohe, C., Kahlert, S., Lobbert, K., Stimpel, M., Karas, R.H., Vetter, H. and Neyses, L. (1997) Cardiac myocytes and fibroblasts contain functional estrogen receptors. FEBS Lett. **416**, 107–112 CrossRef PubMed

6 Mahmoodzadeh, S., Eder, S., Nordmeyer, J., Ehler, E., Huber, O., Martus, P., Weiske, J., Pregla, R., Hetzer, R. and Regitz-Zagrosek, V. (2006) Estrogen receptor α up-regulation and redistribution in human heart failure. FASEB J. **20**, 926–934 CrossRef PubMed

7 Nordmeyer, J., Eder, S., Mahmoodzadeh, S., Martus, P., Fielitz, J., Bass, J., Bethke, N., Zurbrugg, H.R., Pregla, R., Hetzer, R. et al. (2004) Upregulation of myocardial estrogen receptors in human aortic stenosis. Circulation **110**, 3270–3275 CrossRef PubMed

8 Mahmoodzadeh, S., Dworatzek, E., Fritschka, S., Pham, T.H. and Regitz-Zagrosek, V. (2010) 17β-Estradiol inhibits matrix metalloproteinase-2 transcription via MAP kinase in fibroblasts. Cardiovasc. Res. **85**, 719–728 CrossRef PubMed

9 Mendelsohn, M.E. (2002) Protective effects of estrogen on the cardiovascular system. Am. J. Cardiol. **89**, 12E–17E CrossRef PubMed

10 Pedram, A., Razandi, M., Aitkenhead, M., Hughes, C.C. and Levin, E.R. (2002) Integration of the non-genomic and genomic actions of estrogen: membrane-initiated signaling by steroid to transcription and cell biology. J. Biol. Chem. **277**, 50768–50775 CrossRef PubMed

11 Pelzer, T., Loza, P.A., Hu, K., Bayer, B., Dienesch, C., Calvillo, L., Couse, J.F., Korach, K.S., Neyses, L. and Ertl, G. (2005) Increased mortality and aggravation of heart failure in estrogen receptor-β knockout mice after myocardial infarction. Circulation **111**, 1492–1498 CrossRef PubMed

12 Korte, T., Fuchs, M., Arkudas, A., Geertz, S., Meyer, R., Gardiwal, A., Klein, G., Niehaus, M., Krust, A., Chambon, P. et al. (2005) Female mice lacking estrogen receptor β display prolonged ventricular repolarization and reduced ventricular automaticity after myocardial infarction. Circulation **111**, 2282–2290 CrossRef PubMed

13 Babiker, F.A., Lips, D.J., Delvaux, E., Zandberg, P., Janssen, B.J., Prinzen, F., van Eys, G., Grohe, C. and Doevendans, P.A. (2007) Oestrogen modulates cardiac ischaemic remodelling through oestrogen receptor-specific mechanisms. Acta Physiol. **189**, 23–31 CrossRef

14 Fliegner, D., Schubert, C., Penkalla, A., Witt, H., Kararigas, G., Dworatzek, E., Staub, E., Martus, P., Ruiz Noppinger, P., Kintscher, U. et al. (2010) Female sex and estrogen receptor-β attenuate cardiac remodeling and apoptosis in pressure overload. Am. J. Physiol. Regul. Integr. Comp. Physiol. **298**, R1597–R1606 CrossRef PubMed

15 Bernardo, B.C., Weeks, K.L., Pretorius, L. and McMullen, J.R. (2010) Molecular distinction between physiological and pathological cardiac hypertrophy: experimental findings and therapeutic strategies. Pharmacol. Ther. **128**, 191–227 CrossRef PubMed

16 Weeks, K.L., Gao, X., Du, X.J., Boey, E.J., Matsumoto, A., Bernardo, B.C., Kiriazis, H., Cemerlang, N., Tan, J.W., Tham, Y.K. et al. (2012) Phosphoinositide 3-kinase p110α is a master regulator of exercise-induced cardioprotection and PI3K gene therapy rescues cardiac dysfunction. Circ. Heart Fail. **5**, 523–534 CrossRef PubMed

17 McMullen, J.R., Amirahmadi, F., Woodcock, E.A., Schinke-Braun, M., Bouwman, R.D., Hewitt, K.A., Mollica, J.P., Zhang, L., Zhang, Y., Shioi, T. et al. (2007) Protective effects of exercise and phosphoinositide 3-kinase (p110α) signaling in dilated and hypertrophic cardiomyopathy. Proc. Natl. Acad. Sci. U.S.A. **104**, 612–617 CrossRef PubMed

18 Dworatzek, E., Mahmoodzadeh, S., Schubert, C., Westphal, C., Leber, J., Kusch, A., Kararigas, G., Fliegner, D., Moulin, M., Ventura-Clapier, R. et al. (2014) Sex differences in exercise-induced physiological myocardial hypertrophy are modulated by oestrogen receptor β. Cardiovasc. Res. **102**, 418–428 CrossRef PubMed

19 Wang, M., Wang, Y., Weil, B., Abarbanell, A., Herrmann, J., Tan, J., Kelly, M. and Meldrum, D.R. (2009) Estrogen receptor β mediates increased activation of PI3K/Akt signaling and improved myocardial function in female hearts following acute ischemia. Am. J. Physiol. Regul. Integr. Comp. Physiol. **296**, R972–R978 CrossRef PubMed

20 Cleland, J.G., Daubert, J.C., Erdmann, E., Freemantle, N., Gras, D., Kappenberger, L. and Tavazzi, L. (2005) The effect of cardiac resynchronization on morbidity and mortality in heart failure. New Engl. J. Med. **352**, 1539–1549 CrossRef

21 Lang, R.M., Badano, L.P., Mor-Avi, V., Afilalo, J., Armstrong, A., Ernande, L., Flachskampf, F.A., Foster, E., Goldstein, S.A., Kuznetsova, T. et al. (2015) Recommendations for cardiac chamber quantification by echocardiography in adults: an update from the American Society of Echocardiography and the European Association of Cardiovascular Imaging. Eur. Heart J. Cardiovasc. Imaging **16**, 233–270 CrossRef PubMed

22 Bauer, M., Cheng, S., Jain, M., Ngoy, S., Theodoropoulos, C., Trujillo, A., Lin, F.C. and Liao, R. (2011) Echocardiographic speckle-tracking based strain imaging for rapid cardiovascular phenotyping in mice. Circ. Res. **108**, 908–916 CrossRef PubMed

23 Ram, R., Mickelsen, D.M., Theodoropoulos, C. and Blaxall, B.C. (2011) New approaches in small animal echocardiography: imaging the sounds of silence. Am. J. Physiol. Heart Circ. Physiol. **301**, H1765–H1780 CrossRef PubMed

24 Kanno, S., Lerner, D.L., Schuessler, R.B., Betsuyaku, T., Yamada, K.A., Saffitz, J.E. and Kovacs, A. (2002) Echocardiographic evaluation of ventricular remodeling in a mouse model of myocardial infarction. J. Am. Soc. Echocardiogr. **15**, 601–609 CrossRef PubMed

25 Benavides-Vallve, C., Corbacho, D., Iglesias-Garcia, O., Pelacho, B., Albiasu, E., Castano, S., Munoz-Barrutia, A., Prosper, F. and Ortiz-de-Solorzano, C. (2012) New strategies for echocardiographic evaluation of left ventricular function in a mouse model of long-term myocardial infarction. PLoS One **7**, e41691 CrossRef PubMed

26 Mahmoodzadeh, S., Leber, J., Zhang, X., Jaisser, F., Messaoudi, S., Morano, I., Furth, P.A., Dworatzek, E. and Regitz-Zagrosek, V. (2014) Cardiomyocyte-specific estrogen receptor α increases angiogenesis, lymphangiogenesis and reduces fibrosis in the female mouse heart post-myocardial infarction. J. Cell Sci. Ther. **5**, 153 CrossRef PubMed

27 Lips, D.J., Bueno, O.F., Wilkins, B.J., Purcell, N.H., Kaiser, R.A., Lorenz, J.N., Voisin, L., Saba-El-Leil, M.K., Meloche, S., Pouyssegur, J. et al. (2004) MEK1–ERK2 signaling pathway protects myocardium from ischemic injury *in vivo*. Circulation **109**, 1938–1941 CrossRef PubMed

28 Schwartz, R.J. and Yeh, E.T. (2012) Weighing in on heart failure: the role of SERCA2a SUMOylation. Circ. Res. **110**, 198–199 CrossRef PubMed

29 Kranias, E.G. and Hajjar, R.J. (2012) Modulation of cardiac contractility by the phospholamban/SERCA2a regulatome. Circ. Res. **110**, 1646–1660 CrossRef PubMed

30 Periasamy, M., Reed, T.D., Liu, L.H., Ji, Y., Loukianov, E., Paul, R.J., Nieman, M.L., Riddle, T., Duffy, J.J., Doetschman, T. et al. (1999) Impaired cardiac performance in heterozygous mice with a null mutation in the sarco(endo)plasmic reticulum Ca^{2+}-ATPase isoform 2 (SERCA2) gene. J. Biol. Chem. **274**, 2556–2562 CrossRef PubMed

31 Schultz Jel, J., Glascock, B.J., Witt, S.A., Nieman, M.L., Nattamai, K.J., Liu, L.H., Lorenz, J.N., Shull, G.E., Kimball, T.R. and Periasamy, M. (2004) Accelerated onset of heart failure in mice during pressure overload with chronically decreased SERCA2 calcium pump activity. Am. J. Physiol. Heart Circ. Physiol. **286**, H1146–H1153 CrossRef PubMed

32 He, H., Giordano, F.J., Hilal-Dandan, R., Choi, D.J., Rockman, H.A., McDonough, P.M., Bluhm, W.F., Meyer, M., Sayen, M.R., Swanson, E. et al. (1997) Overexpression of the rat sarcoplasmic reticulum Ca^{2+} ATPase gene in the heart of transgenic mice accelerates calcium transients and cardiac relaxation. J. Clin. Invest. **100**, 380–389 CrossRef PubMed

33 Baker, D.L., Hashimoto, K., Grupp, I.L., Ji, Y., Reed, T., Loukianov, E., Grupp, G., Bhagwhat, A., Hoit, B., Walsh, R. et al. (1998) Targeted overexpression of the sarcoplasmic reticulum Ca^{2+}-ATPase increases cardiac contractility in transgenic mouse hearts. Circ. Res. **83**, 1205–1214 CrossRef PubMed

34 Kong, P., Christia, P. and Frangogiannis, N.G. (2014) The pathogenesis of cardiac fibrosis. Cell. Mol. Life Sci. **71**, 549–574 CrossRef PubMed

35 Queiros, A.M., Eschen, C., Fliegner, D., Kararigas, G., Dworatzek, E., Westphal, C., Sanchez Ruderisch, H. and Regitz-Zagrosek, V. (2013) Sex- and estrogen-dependent regulation of a miRNA network in the healthy and hypertrophied heart. Int. J. Cardiol. **169**, 331–338 CrossRef PubMed

36 Thum, T., Gross, C., Fiedler, J., Fischer, T., Kissler, S., Bussen, M., Galuppo, P., Just, S., Rottbauer, W., Frantz, S. et al. (2008) MicroRNA-21 contributes to myocardial disease by stimulating MAP kinase signalling in fibroblasts. Nature **456**, 980–984 CrossRef PubMed

37 Adam, O., Lohfelm, B., Thum, T., Gupta, S.K., Puhl, S.L., Schafers, H.J., Bohm, M. and Laufs, U. (2012) Role of miR-21 in the pathogenesis of atrial fibrosis. Basic Res. Cardiol. **107**, 278 CrossRef PubMed

38 Cardin, S., Guasch, E., Luo, X., Naud, P., Le Quang, K., Shi, Y., Tardif, J.C., Comtois, P. and Nattel, S. (2012) Role for microRNA-21 in atrial profibrillatory fibrotic remodeling associated with experimental postinfarction heart failure. Circ. Arrhythm. Electrophysiol. **5**, 1027–1035 CrossRef PubMed

39 Paris, O., Ferraro, L., Grober, O.M., Ravo, M., De Filippo, M.R., Giurato, G., Nassa, G., Tarallo, R., Cantarella, C., Rizzo, F. et al. (2012) Direct regulation of microRNA biogenesis and expression by estrogen receptor β in hormone-responsive breast cancer. Oncogene **31**, 4196–4206 CrossRef PubMed

40 Nilsson, S., Koehler, K.F. and Gustafsson, J.-Å. (2011) Development of subtype-selective oestrogen receptor-based therapeutics. Nat. Rev. Drug Discov. **10**, 778–792 CrossRef PubMed

Received 28 August 2015/16 November 2015; accepted 25 November 2015
Accepted Manuscript online 25 November 2015, doi: 10.1042/CS20150609

